Journal of Fisheries
Volume 14 Issue 1 April 2026
Peer Reviewed | Open Access

eISSN 2311-3111
pISSN 2311-729X

DOI: https://doi.org/10.17017/j.fish.1146

Original Article

Using brine shrimp to assess the performance of *Annona muricata*–zinc oxide nanoparticles: characterization and evaluation of photocatalytic, antibacterial and antibiofilm properties

Faiz Al Faiz • Rajendran Vijayakumar

Department of Biology, College of Science in Zulfi, Majmaah University, Al Majmaah 11952, Saudi Arabia

Correspondence
Rajendran Vijayakumar; Department of Biology, College of Science in Zulfi, Majmaah University, Al Majmaah 11952, Saudi Arabia.
v.kumar@mu.edu.sa

Manuscript history
Received 12 November 2025 | Accepted 13 December 2025 | Published online 17 December 2025

Citation
Faiz FA, Vijayakumar R (2026) Using brine shrimp to assess the performance of *Annona muricata*–zinc oxide nanoparticles: characterization and evaluation of photocatalytic, antibacterial and antibiofilm properties. Journal of Fisheries 14(1): 141205. DOI: 10.17017/j.fish.1146

Abstract
The development of multifunctional nanoparticles through green synthesis is an important advancement in nanotechnology, addressing the growing need for effective antimicrobial agents against drug-resistant pathogens and efficient photocatalysts for environmental remediation, while also necessitating thorough eco-toxicological assessments to ensure their safe application, particularly in sensitive ecosystems like fisheries. In this study, we investigated the antimicrobial activities, photocatalytic activity and eco-friendly assessment on zooplankton crustacean *Artemia salina* and phytochemical properties of biosynthesized zinc oxide nanoparticles using aqueous fruit extract of *Annona muricata* (Am-ZnO NPs). The synthesized Am-ZnO NPs was characterized using UV–visible spectroscopy, X-ray diffraction (XRD), Fourier transform infrared (FTIR) spectroscopy and transmission electron microscopy (TEM). XRD analysis revealed the crystalline nature of Am-ZnO NPs. TEM analysis showed that the Am-ZnO NPs were spherical in shape with a size between 50 and 100 nm. In addition, Am-ZnO NPs showed antibacterial and antibiofilm activity against multiple drug resistance (MDR) Gram positive, *Enterococcus faecalis* bacteria. Am-ZnO NPs showed significant photocatalytic activity against two different organic dye pollutants namely methylene blue and acridine orange under both sunlight and UV light exposure. Ecotoxicity assessment of Am-ZnO NPs (25, 50, 75, and 100 µg mL^{-1}) showed no toxicity against non-targeted marine crustacean *Artemia salina* at low concentration and slightly toxic at high concentration (100 µg mL^{-1}). Together, the results suggest the potential application of Am-ZnO NPs against multiple drug resistance microbes and photocatalytic activities.

Keywords: *Annona muricata*; antibacterial; antibiofilm; *Artemia salina*; *Enterococcus faecalis*

1 | INTRODUCTION

The management of infectious diseases in human medicine, veterinary practice, and agriculture, including aquaculture, is fundamentally dependent on antimicrobial agents. For more than 50 years, antibiotics have been extensively used in aquaculture, not only for treating active bacterial infections in aquatic species but also for disease prevention and as growth promoters to enhance productivity in yield (Khan *et al*. 2024). This widespread, improper use and incorrect usage of antibiotics is a principal cause of developing antimicrobial resistance, it caused severe economic loss and a critical global health

crisis (Deekshit *et al*. 2022). In the healthcare setup, a great example of the Gram-positive bacterium *Enterococcus faecalis* is a major cause of nosocomial infection, which causes chronic and hard-to-treat infections (Tamrat *et al*. 2025). This problem is compounded by the ability of pathogenic bacteria to form resistant biofilms, which are structured communities encased in a protective extracellular matrix. In aquaculture, biofilm-associated infections lead to significant stock losses and huge economic losses in productivity, while in clinical settings, they cause persistent, recurrent infections that are extremely difficult to eradicate and contribute to high mortality rates (Ramasamy and Lee 2016; Vijayakumar *et al*. 2017). This dual challenge highlights an urgent need for researchers to find out the innovative, effective, and sustainable alternatives to conventional antimicrobials.

In this response, plant-derived phytocompounds have gained considerable attention from worldwide researchers to find out a promising, biocompatible alternatives due to their diverse bioactive properties of phytochemicals (Riaz *et al*. 2023). Among these, *Annona muricata* (also called soursop), a tropical evergreen plant, is notable for its extensive use in ethnomedicine of indigenous people in Africa and South America. It has a wide range of documented therapeutic activities, including anticancer, antimalarial, and antimicrobial effects (Moghadamtousi *et al*. 2015; Patel and Patel 2016). Simultaneously, nanotechnology offers transformative potential for disease control. In recent times, engineered nanoparticles in particular metal nanoparticle, have established a lot of attention from the scientists (Khan *et al*. 2024). Among various nanoparticles, zinc oxide nanoparticles (ZnO NPs) are very important due to their exclusive physicochemical properties, biocompatibility, and regulatory recognition as safe application (Rasmussen *et al*. 2010). These nanoparticles are already utilized in consumer products for their UV-blocking and inherent antimicrobial properties (Newman *et al*. 2009; Hatamie *et al*. 2015). Integrating these fields, the green synthesis of ZnO NPs using plant extracts like *A. muricata* leverages natural phytochemicals as reducing and stabilizing agents, offering an eco-friendly route to functional nanomaterials (Somu and Paul 2019).

However, the safe utilization of nanomaterials in the aquatic ecosystem needs severe ecotoxicological evaluations. For this situation, *Artemia salina* (also called brine shrimp) serves as a vital laboratory model. This microcrustacean, well adapted organism to the harsh conditions of high saline environments, which impose significant survival and reproductive pressures. As an important live feed organism in aquaculture, also widely accpeted as a standard laboratory model organism, particularly in ecotoxicological studies. *Artemia salina* is extensively used to assess the cytotoxicity or bioactivity of both natural and synthetic compounds by various researchers (Rajabi *et al*. 2015; Libralato *et al*. 2016; Lantushenko *et al*. 2023). Despite its frequent use, limited studies have employed *A. salina* to evaluate the biosafety of nanomaterials synthesized using *A. muricata* extracts. Therefore, this study aims to biosynthesize zinc oxide nanoparticles using an aqueous fruit extract of *A. muricata* and evaluate their antibacterial, antibiofilm, and photocatalytic activities. Additionally, the ecotoxicological assessment done with *A. salina* to find out the suitability for potential applications in sustainable aquaculture.

2 | METHODOLOGY

2.1 Sample collection

The fruit of *A. muricata* were brought from the local market in the Al Qassim region of Saudi Arabia. The *A. muricata* fruit was mechanically ground, shade dried, and put through a 50-mesh sieve before being processed. In a Soxhlet apparatus, 50 g of dry powder was filled, and it was sequentially extracted with 90% ethanol (1:10 ratio) for 24 hours. A rotary evaporator was used to concentrate the extract at 400°C (R-3 Rotavapour). The concentrated extract was vacuum-lyophilized at –55°C to produce dry powder. The 6.5 g of dried ethanol extract obtained was stored for phytochemical screening in the refrigerator.

2.2 Preliminary phytochemical analysis of *A. muricata*

Qualitative assessment of terpenoids, steroids, saponins, proteins, flavonoids, carbohydrates, and phenolic compounds in the *A. muricata* fruit extract was determined through preliminary phytochemical analysis.

2.3 Synthesis of *A. muricata* fruit extract coated ZnO NPs

For the synthesis of *A. muricata* fruit extract coated ZnO NPs (Am-ZnO NPs), 50 mL of 0.1 M zinc acetate dihydrate was prepared using deionized water. Upon complete dissolutions, the extract was added dropwise to the solution. The precipitate is formed by continuous stirring at 30 minutes. The pH was adjusted to 5 through the entire process. This mixture was placed on magnetic stirrer at 80°C for 3 hours until white precipitation was formed. This indicates the reduction of zinc oxide. After that, the mixture was centrifuged at 7000 rpm for 10 minutes. The supernatant was discarded, the pellet was rinsed with distilled water. The pellet was transferred to a petri dish and dried in a hot-air oven at 80°C till the water content was fully evaporated. The resulting dry powder was then collected, it was ground on motor pestle to remove any lumps and weighed. This powder was then calcinated (at 300°C) in muffle furnace for complete reduction for 30 minutes (Ramanarayanan *et al*. 2018).

2.4 Physio-chemical characterization of Am-ZnO NPs

2.4.1 UV-visible spectroscopic analysis: For spectroscopic analysis, 1 mL of the Am-ZnO NPs reaction mixture was

withdrawn. Its absorbance was measured using a UV-visible spectrophotometer across a wavelength range of 300 nm to 800 nm. UV-visible spectrum analysis was performed in a UV-visible spectrometer (UV-1800, Shimadzu, Japan).

2.4.2 X-Ray diffraction (XRD) analysis: The crystalline nature of the synthesized Am-ZnO NPs was analyzed using X-ray diffraction (XRD). The nanoparticles were first centrifuged, washed, and air-dried. The resulting powder was then coated onto a glass slide and analyzed using a PAN analytical XRD analyzer (X pert PRO) operating in transmission mode with Cu Kα radiation (λ = 1.5406 Å) at 40 kV and 30 mA.

2.4.3 Fourier transform infrared spectroscopy (FTIR) analysis: Fourier transform infrared (FTIR) spectroscopy was employed to analyze the functional groups of the biosynthesized Am-ZnO NPs. For analysis, two milligrams of Am-ZnO NPs were thoroughly mixed with 200 mg of potassium bromide and pressed into a pellet under hydraulic pressure. The pellet was then placed in the spectrometer sample holder, and the FTIR spectrum was recorded at a resolution of 4 cm^{-1}.

2.4.4 Transmission electron microscopy (TEM) analysis: To determine the grain shape and size of the nanoparticles TEM analysis was carried out. The microscopic structures of nanoparticles were analyzed through TEM analysis.

2.4.5 Bacterial strains: Gram-positive *E. faecalis* bacteria were kept at –80°C in LB broth medium with sterile 80% glycerol. A sterile inoculation needle was used to scrape the frozen surface of the culture, and it was then immediately put into 2 mL of nutritional broth. In an orbital shaker, the bacteria were allowed to grow overnight at 37°C. The well-grown culture was used to examine the antibacterial and antibiofilm activities following incubation.

2.5 Antioxidant activity

2.5.1 2,2-diphenyl-1-picrylhydrazyl (DPPH) assay: The antioxidant capacity of Am-ZnO NPs was evaluated using a DPPH assay. The ability of Am-ZnO NPs-based nanoparticle to scavenge free radicals was evaluated using the stable free radical indicator DPPH. Using ethanol as the medium, 50 mL of 0.1 mM DPPH free radical solution was created. Am-ZnO NPs were added to 100 µL of a DPPH solution at various concentrations (25, 50, 75, and 100 µg mL^{-1}). Ascorbic acid and a DPPH solution without nanoparticles were considered as the positive and negative controls, respectively. To prevent photolytic degradation, the microplate was wrapped in aluminum foil and incubated in the dark. The titer plate reader set to 517 nm was used to detect absorbance after 30 minutes. The free radical scavenging activity was calculated using the following formula,

% of Inhibition= [(A blank – A sample)/A blank] × 100

Where A blank is an absorbance without samples and A sample is an absorbance in the presence of samples.

2.6 Antibacterial assay

The antibacterial activity of Am-ZnO NPs against the Gram-positive bacterium *E. faecalis* was evaluated using the agar well diffusion method, as described by Vinotha *et al*. (2019) with slight modifications. Concisely, nutrient agar plates were prepared by pouring approximately 20 ml of molten agar into each Petri dish and allowing it to solidify. After solidification, a standardized microbial suspension (10 µL) were inoculated over the culture media using sterile cotton swabs. Wells of uniform diameter were then aseptically created in the inoculated culture plate using a sterile well borer. Subsequently, different concentrations of Am-ZnO NPs (25, 50, 75, and 100 µg mL^{-1}) were introduced into the corresponding wells. The plates were incubated at 37°C for 24 hours, after which the diameters of the zones of inhibition of each were measured, recorded the results in millimeters.

2.7 Antibiofilm activity

The *in vitro* antibiofilm activity of Am-ZnO NPs was tested against bacterial biofilms grown on glass pieces. For this assay, a bacterial strain of *E. faecalis* was cultured in a 24-well plate. To provide a surface for adherence, small glass pieces (1×1 cm) cut from a glass slide were placed in each well. A 10 µL aliquot of the culture was added to the respective wells, which were then incubated at 37°C for 24 hours to allow biofilm formation. The developed biofilms were then treated with Am-ZnO NPs at various concentrations (25, 50, 75, and 100 µg mL^{-1}), and the plate was incubated overnight. Following incubation, the spent broth was carefully aspirated, and the biofilms were stained with crystal violet for one hour. After staining, excess dye was removed, and the bound crystal violet was solubilized with acetone for spectrophotometric quantification. Finally, the glass pieces were observed under a light microscope to visualize biofilm disruption.

2.8 Photocatalytic activity of Am-ZnO NPs

The photocatalytic evaluation checker models are methylene blue and acridine orange as the test dye to be degraded (Frunza *et al*. 2018). 10 ppm of respective dyes was treated with 10 mg mL^{-1} of Am-ZnO NPs under sunlight and UV irradiation. The degradation of total organic carbon from the selected dye pollutant was estimated at different time intervals. The percentage of degradation was calculated as follows,

% of degradation = C0 – Ct / C0 × 100

Here, C0 and Ct stands for absorbance of initial and final concentration of dye respectively. Moreover, the pseudo

first order kinetics was adopted to calculate the constant rate kinetics.

Pseudo first order kinetics = In [C0 / Cf] = kt

Here, C0 and Cf stand for initial and final dye concentration; k means degradation constant; t means time.

2.9 Toxicity against non-targeted organisms

Toxicity against non-targeted organisms refers to the harmful effects of a substance on organisms other than the intended target. Non-target organisms encompass beneficial species, including pollinators, natural predators, and those essential for ecosystem functioning and commercial activities of fisheries. *Artemia salina*, also known as brine shrimp, serves as a well-established model organism in toxicological studies due to its sensitivity to various environmental stressors and chemicals (Rajabi *et al*. 2015). Additionally, *A. salina* is an essential component of the food chain, serving as a primary live feed in aquaculture and a natural food source for various larval fish in wild fisheries. Evaluating the toxicity on *A. salina* thus aids in understanding potential bioaccumulation and biomagnification effects, which can have extensive consequences on higher trophic levels and the sustainability of aquatic food resources (Libralato *et al*. 2016).

2.9.1 Culture of *A. salina*: *Artemia salina* cysts were bought commercially (Ocean Star International) and stored at 4°C prior to use. The organisms were cultured according to the standard protocol established by Veeramani and Baskaralingam (2011). In this part of experiment, artificial seawater (35 g L^{-1} of sodium chloride in sterile distilled water) was prepared and strictly maintained the environmental conditions such as salinity (32 ppt), pH (7.8 – 8.0), temperature (30°C), and photo period exposure to light (16 hours) and dark (8 hours) conditions. The culture was provided with continuous illumination and aeration via air spargers. Upon the introduction of the cysts, hatched nauplii emerged within 24 hours, after which any remaining unhatched cysts were removed. The nauplii were fed a diet of microalgae at regular intervals, and 90% of the culture water was renewed daily to maintain water quality.

2.9.2 Acute toxicity: *Artemia salina*'s nauplii stage was used for the investigation of acute toxicity (48 hours). Different concentrations (25, 50, 75, 100 µg mL^{-1}) of Am-ZnO NPs were used for the experimentation. In 24 well plates, second instar nauplii were added for acute toxicity testing. 10 brine shrimps were added in each well and Am-ZnO NPs were administered to the treated group in each experimental study; there were none in the control group. Three duplicates of each experiment were run. Animals that were immobile following acute exposure were counted under a microscope.

2.10 Biochemical assays-metabolic and antioxidant enzymes

In order to study the level of toxicity exhibited by the Am-ZnO NPs, biochemical assays were carried out on test organisms *A. salina*.

2.10.1 Preparation of homogenate of the organisms: Using a mortar and pestle the test organisms *A. salina* were collected and ground using PBS to make the homogenate. It was subsequently centrifuged at 10000 rpm for 15 minutes. The WHO-recommended standard procedure was utilised to conduct biochemical analysis on the supernatant. In the control and treatment (exposure Am-ZnO NPs) groups of *A. salina*, the biochemical indicators of antioxidant enzymes including superoxide dismutase (SOD), catalase (CAT), glutathione peroxidase (GPx), and glutathione S-transferase (GST) were measured.

2.10.2 Superoxide dismutase activity: SOD activity was evaluated using the Suzuki (2000) technique, which measures absorbance at 560 nm. Variations of SOD activity were determined in *A. salina* treated with Am-ZnO NPs. The amount of SOD that can catalyse the conversion of 1 µ mol of substrate per minute is given as U mg-L, where one unit (U) is equal to the amount of SOD.

2.10.3 Catalase activity: The CAT activity was performed in accordance with the technique of Cohen *et al*. (1970) protocol to analyse the absorbance variation between treated and untreated Am-ZnO NPs. By analysing the breakdown of hydrogen peroxide (H_2O_2) from the decrease in absorption at 405 nm, a standard curve was established. Activity of CAT was determined as U mg L^{-1}.

2.10.4 Glutathione peroxidase activity: According to Rotruck *et al*. (1973), GPx activity was measured in which NADPH oxidation occurs in the presence of H_2O_2. GPx was read at 420 nm using a microplate reader. To compare the impact of treated (Am-ZnO NPs) and untreated, GPx activity was quantified in terms of U mg-L protein.

2.10.5 Glutathione -S- transferase activity: Using 1-chloro2, 4-dinitrobenzene (CDNB) as the substrate, the change in absorbance of the GST activity was done at 340 nm to read out the absorbance difference between Am-ZnO NPs treated and control, which was estimated as U mg-L protein (Gopi *et al*. 2019).

2.11 Data analysis

Prior to starting statistical analysis, the work was planned using an unconditionally randomised approach, therefore the data were checked for normality using the Shapiro-Wilk test and the homogeneity of variance was determined using the Levene's test. To investigate the effects of time and concentration of Am-ZnO NPs on biochemical

parameters in *A. salina*, the results (mean standard deviation) were analysed in one-way ANOVA followed by Tukey's HSD test. The test was utilized to find significant differences between the Am-ZnO NPs treated and control groups. All of the statistical analyses' comparing graphics were created using MS-Excel.

3 | RESULTS

3.1 Characterization of Am-ZnO NPs

The synthesis of *A. muricata* fruit extract mediated zinc oxide nanoparticles was successfully achieved through co-precipitation method. The color of solution altered from brown to pale yellowish white colour reaction, indicated the formation of Am-ZnO NPs. UV-Visible absorption spectra of the coated ZnO NPs were achieved after 4 hours at 150°C. Am-ZnO NPs exhibited a characteristic UV absorption spectrum with a peak at 350 nm (Figure 1a), which corresponds to the fundamental band gap absorption of ZnO nanoparticles. FTIR spectrum of Am-ZnO NPs is shown in the Figure 1b. The broad absorption band showed can be assigned to O-H bonded stretching alcohol groups. The middle peak displayed can be assigned to alcohols and phenols, can be related to the presence of amines, responsible for the presence of alkene group. The absorption band is probably linked to aromatics while could be halogen group. These functional groups play an important role in reduction the NPs. TEM analysis revealed that the Am-ZnO NPs has spherical structure (Figure 1c) and the size ranges between 50 – 100 nm. The XRD pattern revealed the formation of crystalline nature of Am-ZnO NPs (Figure 1d). The XRD spectrum showed strong diffraction peaks at which are showed consequence to crystal planes.

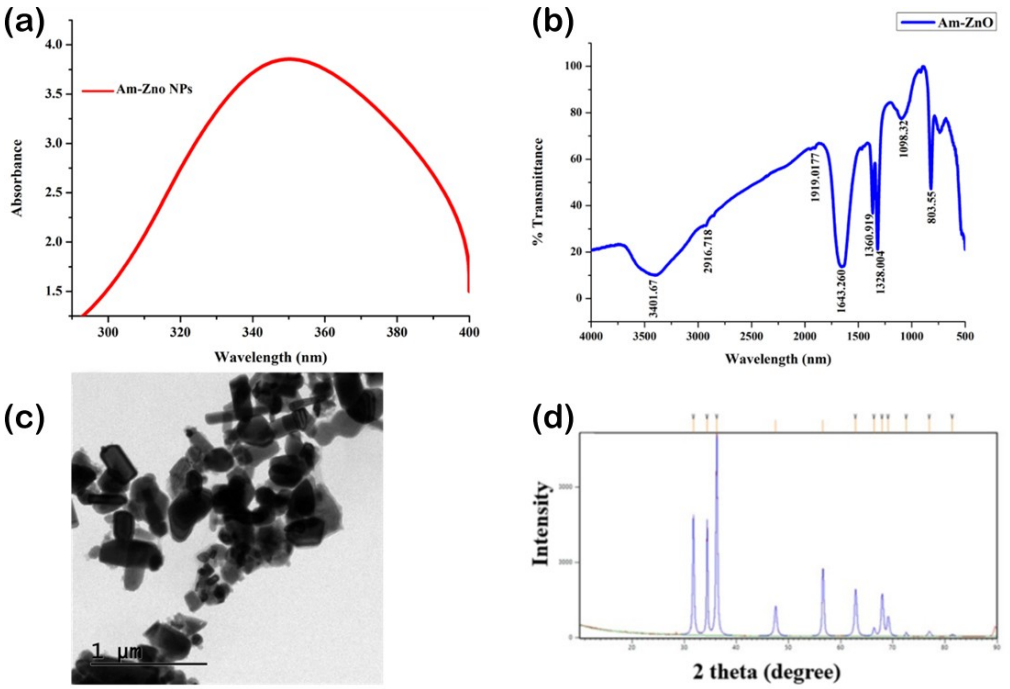

FIGURE 1 a) UV-Vis spectrophotometer (UV), b) Fourier Transform Infrared Spectroscopy (FTIR), c) Transmission Electron Microscopic images (TEM), d) X-ray diffraction (XRD) of Am-ZnO NPs.

3.2 Preliminary phytochemical screening

Simple biochemical assays were employed to determine the ethanolic fruit extract of *A. muricata* for various phytochemicals. The analysis confirmed the presence of multiple therapeutically relevant compounds, including alkaloids, terpenoids, tannins and flavonoids. In contrast, saponins were not detected (Table 1).

3.3 Antioxidant activity

The DPPH assay was used to check the antioxidant activity of Am-ZnO NPs, and the results are shown in Figure 2. The statistics demonstrate that when fruit extract of *A. muricata* content increases, the scavenging percentage also rises. The fruit extract of *A. muricata* is an effective antioxidant. Data utilising ascorbic acid as a standard reference material demonstrates that antioxidant activity rises with concentration (75, and 100 µg mL^{-1}). Increased Am-ZnO NPs concentration of 100 µg L^{-1} shows increased antioxidant activity comparing to the lowest exposure group of 25 µg L^{-1}.

3.4 Antibacterial assay using agar well diffusion method

The agar well diffusion method was used to evaluate the antibacterial properties of the Am-ZnO NPs. According to the findings, the tested strain of *E. faecalis* was effectively controlled by the fruit extract of Am-ZnO NPs (Figure 3). Overall, the findings demonstrated a concentration-dependent inhibitory effects of the fruit extract of Am-ZnO NPs increased against *E. faecalis*. Increased concentration of 100 µg L^{-1} shows increased antibacterial activity

comparing to the lowest exposure group of 25 µg L^{-1} against the Gram-positive *E. faecalis*.

TABLE 1 Phytochemical screening of the fruit extract of *Annona muricata*.

Sl. No	Phytochemical	Presence/Absence
1.	Protein	Present
2.	Saponins	Present
3.	Flavonoids	Present
4.	Phenol	Present
5.	Terpenoids	Present
6.	Steroids	Absent
7.	Glycosides	Present
8.	Carbohydrate	Present

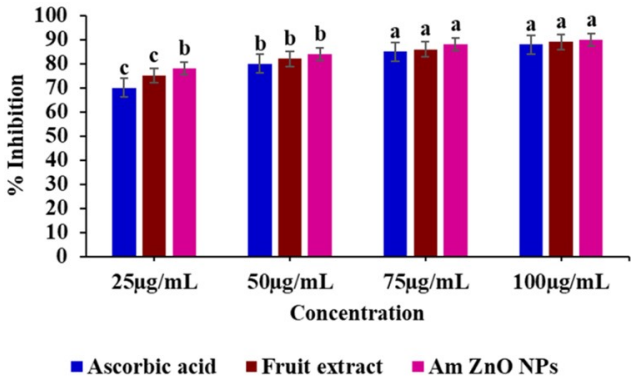

FIGURE 2 Antioxidant activity by DPPH method at different concentrations of *Annona muricata* extract and AM-ZnO NPs.

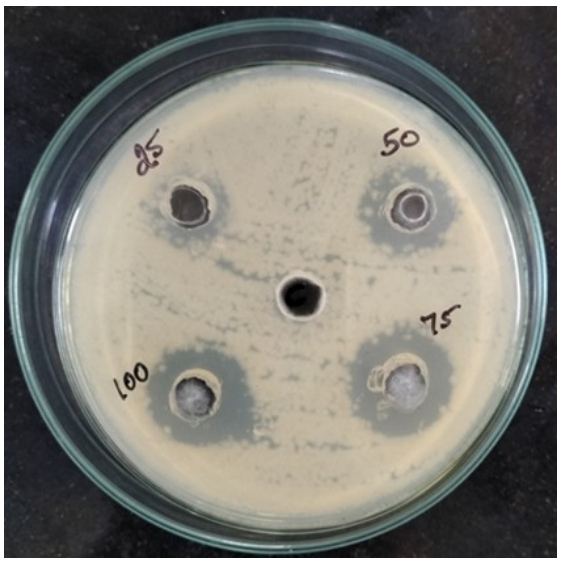

FIGURE 3 Antibacterial activity of Am-ZnO NPs at different concentrations (25, 50, 75, 100 µg/mL) against *Enterococcus faecalis*.

3.5 Antibiofilm activity

The microscopic images provided visual observations of the biofilm formed by *E. faecalis* bacteria after exposure to Am-ZnO NPs (Figure 4). Instead, an untreated sample showed a dense and compact biofilm structure. The findings showed that Am-ZnO NPs (100 µg mL^{-1}) significantly decreased biofilm formation in *E. faecalis* bacteria without cell death. It demonstrates that Am-ZnO NPs completely disperses the biofilm architecture in the treated sample by loosening the microbial colonies. Both qualitative and quantitative analysis' findings support the idea that Am-ZnO NPs prevents the tested pathogens' early attempts to build biofilms.

3.6 Photocatalytic activity

Am-ZnO NPs efficiently reduces the amount of total organic carbon (TOC) that occurs in the methylene blue. In the case of acridine orange, 98.92% of TOC was decreased under the exposure of sunlight (Figure 5a) respectively. Under the exposure of UV light, the degraded TOC was 85.06% (Figure 5b) sequentially. Comparatively, 94.82% of TOC of methylene blue was exceptionally reduced under sunlight radioactivity after 90 min (Figure 5c) respectively. Whereas the TOC of methylene blue under UV light exposure was 84.24% (Figure 5d) respectively. The photocatalytic investigation revealed that these Am-ZnO NPs effectively degrade MB and AO when exposed to sun and ultraviolet rays.

3.8 Biochemical assays-metabolic and antioxidant enzymes

3.8.1 Superoxide dismutase activity: Superoxide dismutase (SOD) serves as a primary defence enzyme, protecting cells by catalyzing the dismutation of superoxide free radicals into molecular oxygen and hydrogen peroxide. In this study, a statistically significant difference ($p \leq 0.05$) in SOD activity was observed in *A. salina* exposed to Am-ZnO NPs compared to the control group (Figure 6). Specifically, the exposed organisms exhibited a marked decrease in SOD activity (Figure 7a). This reduction likely results from the overproduction of reactive oxygen species (ROS) induced by nanoparticle exposure. The resulting oxidative burden may deplete the enzyme as it neutralizes excess free radicals, thereby activating the broader antioxidant system as a compensatory mechanism to mitigate oxidative stress.

3.8.2 Catalase activity

Catalase (CAT) is an essential intracellular antioxidant enzyme that protects cells from oxidative damage by catalyzing the decomposition of hydrogen peroxide into water and molecular oxygen, thereby maintaining cellular redox homeostasis. In this study, a statistically significant difference ($p \leq 0.05$) in catalase activity was observed in *A. salina* exposed to various concentrations of Am-ZnO NPs compared to the control group. Specifically, catalase activity increased in *A. salina* with rising concentrations of Am-ZnO NPs (Figure 7b). This upregulation is likely a

compensatory response to elevated levels of ROS induced by nanoparticle exposure. The heightened enzyme activity functions to neutralize excess hydrogen peroxide, thereby protecting the organisms from oxidative stress.

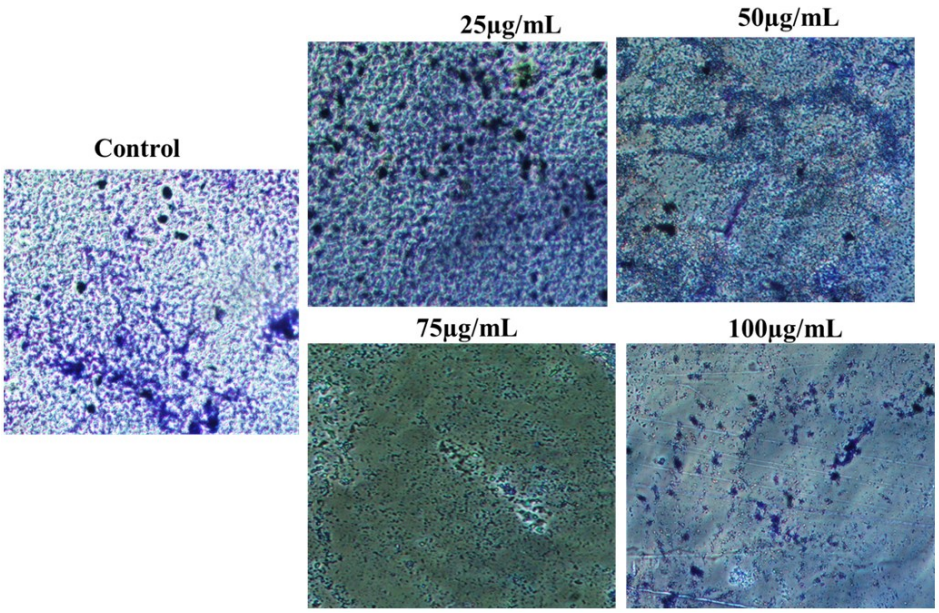

FIGURE 4 Antibiofilm activity of Am-ZnO NPs at different concentrations (25, 50, 75, 100 µg/mL) against *Enterococcus faecalis*.

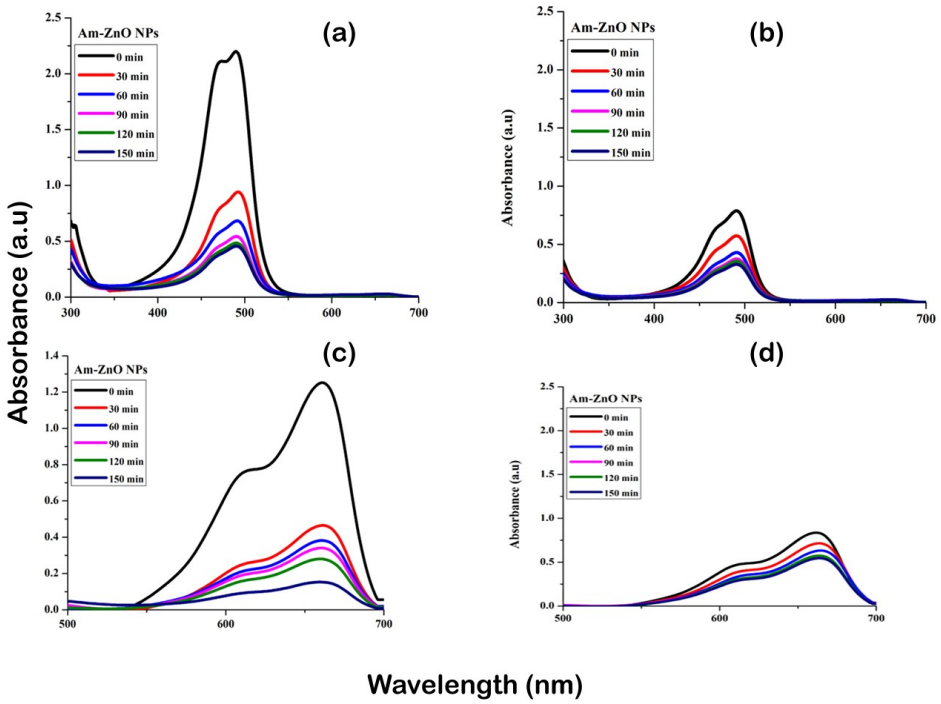

FIGURE 5 Degradation of a) acridine orange dye at sunlight b) UV light exposure c) methylene blue at sunlight d) UV light exposure of Am-ZnO NPs.

3.8.3 Glutathione peroxidase activity

Glutathione peroxidase (GPx) is a class of antioxidant enzymes responsible for scavenging free radicals, thereby aiding in maintaining redox balance, supporting intracellular homeostasis, and preventing lipid peroxidation. *A. salina* exposed to Am-ZnO NPs displayed no significant alteration ($p > 0.05$) in glutathione peroxidase activity between the control and treated groups. (Figure 7c).

3.8.4 Glutathione -S- transferase activity

Glutathione-S-transferase (GST) is an antioxidant enzyme that protects cells from oxidative damage by using reduced glutathione as a co-factor. It functions by neutralizing xenobiotic pollutants and is also involved in the metabolism of lipid oxidation products. In this study, GST activity significantly decreased in the tissues of *A. salina* experimented with the Am-ZnO NPs compared with non-

treated control (Figure 7d). This effect is caused by oxidative damage within their tissues. Furthermore, the activity of this enzyme increases significantly during stress to increase the rate of detoxification process.

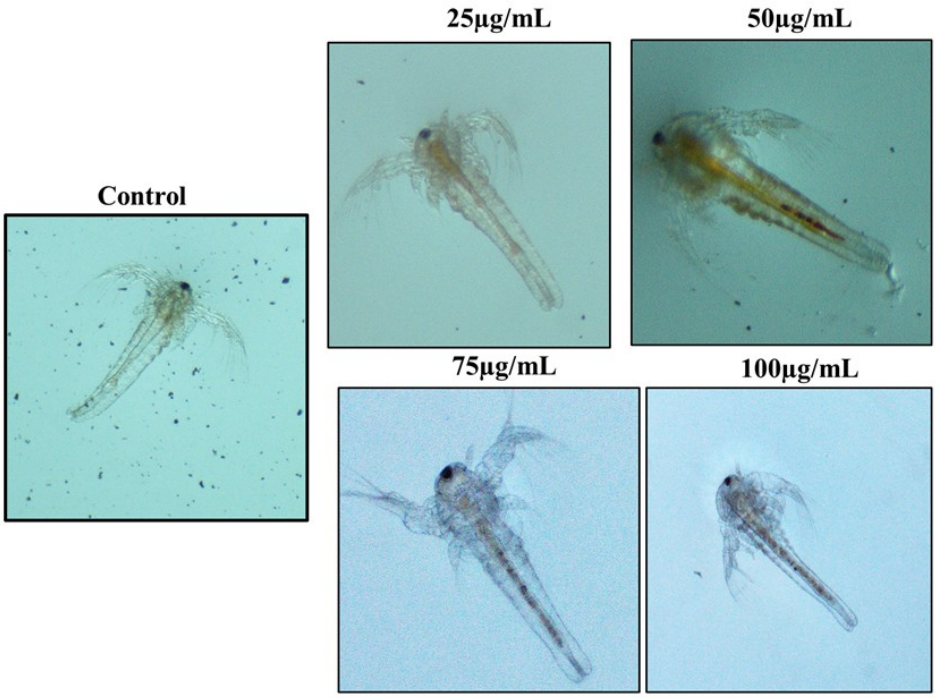

FIGURE 6 Toxicity analysis of Am-ZnO NPs at different concentrations (25, 50, 75, 100 µg/mL) against *Artemia salina*.

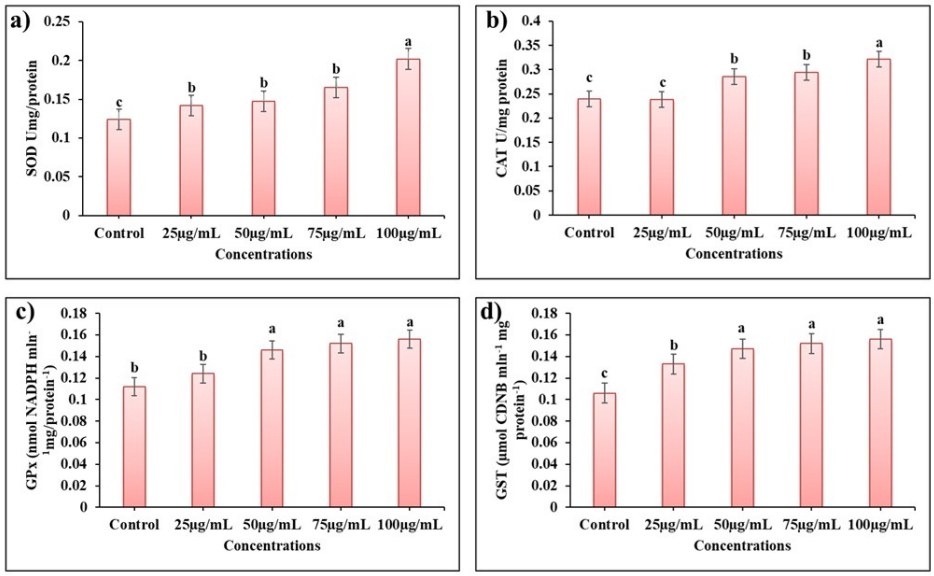

FIGURE 7 a) Superoxide dismutase, b) catalase, c) glutathione peroxidase, d) glutathione-S-transferase in *A. salina* exposed to various concentrations of Am-ZnO NPs at different concentrations (25, 50, 75, 100 µg/mL). The data are represented as mean ± S.D. The treatment groups, values obtained were significantly different ($p \leq 0.05$) as per one -way ANOVA followed by Tukey's HSD test.

4 | DISCUSSION

Recent years have seen growing scientific interest in herbal plant *A. muricata* due to its vast pharmacological activities, particularly its anticancer and antimalarial properties. Beyond human health applications, its potential as a natural antimicrobial agent in sustainable aquaculture and fisheries management has also gained recognition (Moghadamtousi *et al*. 2015). In this study, phytochemical analysis of the aqueous fruit extract of *A. muricata* confirmed the presence of terpenoids, steroids, saponins, proteins, flavonoids, carbohydrates, and phenols. These findings align with previous research; for instance, Sabapati *et al*. (2019) also reported the presence of alkaloids, glycosides, and flavonoids in the ethanolic fruit extract of *A. muricata*. The outcome of this study indicated the existence of substances with therapeutic activity, including tannins, alkaloids, terpenoids, and flavonoids. Saponins, however, were discovered to be lacking. In the majority of researchers, the plant mediated synthesis of nanoparticles was confirmed by UV spectroscopy, followed by TEM, FTIR, and XRD. The shape, size and surface morphology played a vital role in their chemical proper-

ties. Hence in the present study, we have explored the biological synthesis of ZnO NPs by using the *A. muricata* and characterized through UV, XRD, FTIR and TEM analysis. The formation of Am-ZnO NPs was confirmed through visual assessment. The colour of mixture reaction was changed from deep to a pale yellowish white colour during the reaction, indicating the reduction of zinc oxide into Am-ZnO NPs. The absorption spectrum of Am-ZnO NPs is exhibits a strong absorption band at about 350 nm. The spectrum usually shows a distinct peak in the range of 350-450 nm, specific for ZnO NPs. The absorption peak observed at 350 nm corresponds to the excitation of valence electrons within the zinc oxide crystal lattice, confirming that the synthesized nanoparticles absorb light in the ultraviolet region (Huang *et al*. 2006). The antioxidant capability of the Am-ZnO NPs was tested against DPPH. The ROS are unstable free radicals generated as by-products of metabolic reactions and various cellular processes. Their instability arises from unpaired electrons in their outer shell, which drives them to react with and break down vital macromolecules, potentially leading to cell death. While ROS play a crucial role in cellular signaling and cell cycle regulation, their overproduction can lead to oxidative stress. Antioxidants function by scavenging these free radicals, thereby neutralizing ROS and preventing oxidative damage. Am-ZnO NPs demonstrated notable antioxidant capacity, as evidenced by their effective scavenging of DPPH free radicals. Similarly, increased antioxidant potential was observed in *A. muricata* leaf extract by Hasmila *et al*. (2019).

Antibacterial resistance is one of the major challenges in modern medicine. Given their documented antimicrobial properties, plant extracts are considered a promising alternative for controlling infectious diseases. Specifically, the fruit extract of *A. muricata* has demonstrated broad-spectrum antibacterial activity against both Gram-positive and Gram-negative bacteria. The antimicrobial compounds such as acetogenins, alkaloids, and flavonoids, can directly inhibit bacterial growth and viability, which indirectly affects biofilm formation and maintenance. It will induce oxidative stress within bacterial cells that leads to the generation of ROS causing damage to the bacterial cell membrane, DNA, and proteins. Oxidative stress disrupts the physiological processes of biofilm bacteria and weakens their ability to form and maintain a biofilm. The antibacterial and antibiofilm activity of the Am-ZnO NPs was carried out on Gram positive *E. faecalis*. The agar well diffusion method showed that highest concentration of the Am-ZnO NPs act as effective antibacterial agent compared to control. Antibiofilm activity of the fruit extract of *A. muricata* was also assessed. The biofilms are usually formed as a mechanism to cop adverse conditions and its support bacterial resistance towards antibiotics (Hsueh *et al*. 2015). Bacterial biofilms rely on cell-to-cell communication through a process called quorum sensing to coordinate their growth and virulence. *A. muricata* has been found to interfere with quorum sensing systems, inhibiting the production of signaling molecules that are essential for biofilm formation. In addition, *A. muricata* extracts have been shown to inhibit the adhesion of bacteria to surfaces, preventing the initial step of biofilm formation as they contain various bioactive compounds, including enzymes such as proteases and glycosidases, which can degrade the extracellular matrix of biofilms. The extracellular matrix provides structural support and protection to biofilm bacteria. By degrading this matrix, it disrupts the integrity of the biofilm and makes the bacteria more vulnerable to antimicrobial agents. In our study, microscopic analysis confirmed that Am-ZnO NPs achieved complete disruption of the biofilm architecture by significantly reducing the number of micro-colonies in the treated samples. Together, the antibacterial and antibiofilm assays indicate that Am-ZnO NPs effectively inhibit biofilm formation in Gram-positive bacteria. Our findings are supported by Silva *et al*. (2021), who reported potent antibacterial activity of Am-ZnO NPs against *Staphylococcus aureus* and *Escherichia coli*.

Photocatalytic activity of synthesised Am-ZnO NPs is determined by degrading methylene blue and acridine orange under sunlight and UV. Am-ZnO can serve as effective photocatalysts for environmental remediation purposes. The photocatalytic degradation mechanism of plant-based nanoparticles such as titanium dioxide, zinc oxide and iron oxide were reported recently. In the present study, the synthesised Am-ZnO nanoparticles shows a high surface area and possess active sites that can adsorb the dye molecules onto their surface. When exposed to light, Am-ZnO NPs absorb photons and undergo excitation, leading to the generation of electron-hole pairs. This excitation is typically caused by the bandgap energy of the nanoparticles. The valence band electrons are excited to the conduction band, leaving behind positively charged holes in the valence band. The electrons and holes generated will participate in redox reactions. The electrons in the conduction band react with oxygen or water molecules adsorbed on the nanoparticle surface, producing ROS such as hydroxyl radicals (•OH) or superoxide radicals ($\bullet O_2^-$). These ROS are highly reactive and play a vital role in the degradation process of dye. The generated ROS are responsible for the degradation of the adsorbed dye molecules. The ROS attack the dye molecules, leading to the breaking of chemical bonds and the conversion of complex organic compounds into simpler, less harmful products. This degradation process involves oxidation, reduction, or other chemical reactions, depending on the nature of the dye. The slow transition of the dye solution's colour from dark to colourless allowed for the visual identification of dye degradation. As a result, they can be applied in the fabric and water treatment sectors. The recombination of electron-hole pairs is a competing pro-

cess that reduces the efficiency of photocatalysis. Strategies to minimize charge carrier recombination, such as doping Am-ZnO NPs with other elements or modifying its surface, enhance photocatalytic activity. The kinetics of photocatalytic degradation of dyes by Am-ZnO NPs depend on factors such as the concentration of dye molecules, intensity and wavelength of light, surface area and morphology of Am-ZnO NPs, and the presence of electron donors or scavengers (Rajesh *et al*. 2019). The results revealed that Am-ZnO NPs exhibited better photocatalytic activity by using sunlight illumination when compared to that of UV light. Owing to presence of both UV and visible components in the sunlight, it can excite more electrons compared to UV-light alone, hence, sunlight illumination generates overall ROS production rate. In support of the present study, Raj *et al*. (2021) determined a photocatalytic efficiency of 98% for Acid Red dye degradation after ZnO NPs exposure and proved green synthesized ZnO NPs exhibited better photocatalytic activity. Hence, they can be incorporated in water treatment plants and textile industries for removing dye pollutants. The outcomes clearly point to ZnO NPs beneficial involvement in the photocatalytic treatment of hazardous pollutants derived from the clothing and textile sectors.

Focus on the impact of Am-ZnO NPs on the ecosystem is vital to assess the risks that might arise as a result of the plant compounds. The present study focused on the toxicity assessments through enzyme activity on sensitive freshwaters, marine and terrestrial life forms. Ecotoxicity assessment against non-targeted marine crustaceans holds significant implications for environmental applications. As these organisms occupy vital ecological niches and serve as foundational species in marine ecosystems, assessing their sensitivity to various pollutants provides critical insights into the overall health of marine environments. Understanding the effects of contaminants on crustaceans can inform regulatory frameworks, guiding pollution mitigation strategies and the development of environmentally friendly practices. Moreover, ecotoxicity assessments offer a means to evaluate the efficacy of current wastewater treatment methods and the potential risks associated with emerging pollutants, facilitating informed decision-making for sustainable marine resource management and conservation efforts. By safeguarding the health of non-targeted marine crustaceans, these assessments contribute to the preservation of biodiversity and the long-term sustainability of coastal and oceanic ecosystems. It can be concluded from the results that the Am-ZnO NPs tested on non-targeted organisms belonging to habitats *A. salina* showed no toxicity.

Superoxide dismutase (SOD) is a crucial primary defense enzyme that protects cells from oxidative damage by neutralizing superoxide radicals, converting them into hydrogen peroxide and molecular oxygen via a dismutation reaction (Bhagat *et al*. 2016). In the present study, SOD activity was significantly lower in Am-ZnO NP-exposed *A. salina* compared to the control group. Catalase is another essential intracellular antioxidant enzyme that detoxifies hydrogen peroxide (Trestrail *et al*. 2020), converting it into water and oxygen to prevent oxidative damage and maintain cellular homeostasis. In contrast to SOD, catalase activity was significantly elevated in the treated organisms compared to the control. Similarly, the phase II detoxification enzyme glutathione-S-transferase (GST) protects cells from oxidative stress by utilizing reduced glutathione as a co-factor to neutralize xenobiotic compounds and is involved in the metabolism of lipid oxidation products (Trestrail *et al*. 2021). In this study, GST activity, decreased gradually in treated group compared to the control group. Similar results were obtained by Muthu and Durairaj (2015). Thus, overall study took a holistic approach in assessing the potential biological applications of Am-ZnO NPs by taking the ecological risks into consideration. The fruit extract of Am-ZnO NPs could be evaluated for antidiabetic, anti-inflammatory and anticancerous properties in future.

5 | CONCLUSIONS

Overall, the present study focused on the extraction and synthesis of Am-ZnO NPs and determined the efficacy towards antibacterial activity on biofilm-forming microbial pathogens, finding their antioxidant activity. We conclude that Am-ZnO NPs shows good antibacterial and antibiofilm activity on Gram positive bacteria. We also analyzed the impact of a single Am-ZnO NP treatment on biofilm architecture using microscopy. Am-ZnO NPs expressed well established photocatalytic activity against different organic dye pollutants namely methylene blue and acridine orange under both sunlight and UV light exposure. Furthermore, Am-ZnO NPs have not shown any acute toxicity to *A. salina* appealing its safety to aquatic environments. The toxicity analysis on the non-target *A. salina* reveal that Am-ZnO NPs is less toxic at higher concentrations. These findings suggest that multifunctional Am-ZnO NPs, synthesized using a naturally occurring plant extract, represent a promising eco-friendly alternative to conventional chemical methods for antimicrobial and photocatalytic applications, given their lower ecotoxicity and higher biocompatibility at environmentally relevant doses. In conclusion, the biosynthesized Am-ZnO NPs show considerable potential as a sustainable agent for antimicrobial, antibiofilm, antioxidant, and photocatalytic applications in biomedical and environmental remediation, including sustainable aquaculture and fisheries management.

Future directions in this area may involve the development of sustainable synthesis methods, the integration of Am-ZnO NPs into multifunctional materials, and the establishment of rigorous regulatory frameworks to ensure safe deployment. Overall, navigating the broader

implications of Am-ZnO NPs requires a multidisciplinary approach that addresses scientific, ethical, and societal considerations to unlock their full potential while mitigating associated risks.

ACKNOWLEDGEMENTS

The author extends the appreciation to the Deanship of Postgraduate Studies and Scientific Research at Majmaah University for funding this research work through the project number R-2025-2201.

CONFLICT OF INTEREST

The authors declare that they have no known competing financial interests or personal relationships that could have appeared to influence the work reported in this paper.

AUTHORS' CONTRIBUTION

Faiz Al Faiz: Methodology, Validation, Writing Rajendran Vijayakumar: Conceptualization, Methodology, Writing - Review & Editing, Visualization

DATA AVAILABILITY STATEMENT

The data that support the findings of this study are available on request from the corresponding author, R. Vijayakumar.

REFERENCES

Bhagat J, Ingole BS, Singh N (2016) Glutathione S-transferase, catalase, superoxide dismutase, glutathione peroxidase, and lipid peroxidation as biomarkers of oxidative stress in snails: a review. Invertebrate Survival Journal 13(1): 336–349.

Cohen G, Dembiec D, Marcus J (1970) Measurement of catalase activity in tissue extracts. Analytical Biochemistry 34: 30–38

Deekshit VK, Maiti B, Kumar BK, Kotian A, Pinto G, … Karunasagar I (2022) Antimicrobial resistance in fish pathogens and alternative risk mitigation strategies. Reviews in Aquaculture 15(2): 531–552.

Frunza L, Diamandescu L, Zgura I, Frunza S, Ganea CP, … Birzu M (2018) Photocatalytic activity of wool fabrics deposited at low temperature with ZnO or TiO_2 nanoparticles: methylene blue degradation as a test reaction. Catalysis Today 306: 251–259.

Gopi N, Vijayakumar S, Thaya R, Govindarajan M, Alharbi NS, … Vaseeharan B (2019) Chronic exposure of *Oreochromis niloticus* to sub-lethal copper concentrations: effects on growth, antioxidant, non-enzymatic antioxidant, oxidative stress and non-specific immune responses. Journal of Trace Elements in Medicine and Biology 55: 170–179.

Hasmila I, Natsir H, Soekamto NH (2019) Phytochemical analysis and antioxidant activity of soursop leaf extract (*Annona muricata* Linn.). Journal of Physics: Conference Series 1341: 032027.

Hatamie A, Khan A, Golabi M, Turner APF, Beni V, … Willander M (2015) Zinc oxide nanostructure-modified textile and its application to biosensing, photocatalysis, and as antibacterial material. Langmuir 31(39): 10913–10921.

Hsueh YH, Ke WJ, Hsieh CT, Lin KS, Tzou DY, Chiang CL (2015) ZnO nanoparticles affect *Bacillus subtilis* cell growth and biofilm formation. PLoS ONE 10(6): e0128457.

Huang GG, Wang CT, Tang HT, Huang YS, Yang J (2006) ZnO nanoparticle-modified infrared internal reflection elements for selective detection of volatile organic compounds. Analytical Chemistry 78(7): 2397–2404.

Khan SK, Dutta J, Ahmad I, Rather MA (2024) Nanotechnology in aquaculture: transforming the future of food security. Food Chemistry: X 24: 101974.

Lantushenko AO, Meger YV, Gadzhi AV, Anufriieva EV, Shadrin NV (2023) Unique haplotypes of *Artemia salina* (crustacea, branchiopoda, anostraca) in hypersaline lake Sasyk-Sivash (Crimea). Inland Water Biology 16: 884–891.

Libralato G, Prato E, Migliore L, Cicero AM, Manfra L (2016) A review of toxicity testing protocols and endpoints with *Artemia* spp. Ecological Indicators 69: 35–49.

Moghadamtousi SZ, Fadaeinasab M, Nikzad S, Mohan G, Ali HM, Kadir HA (2015) *Annona muricata* (Annonaceae): a review of its traditional uses, isolated acetogenins and biological activities. International Journal of Molecular Sciences 16(7): 15625–15658.

Muthu S, Durairaj B (2015) Evaluation of antioxidant and free radical scavenging activity of *Annona muricata*. European Journal of Experimental Biology 5(3): 39–45.

Newman MD, Stotland M, Ellis JI (2009) The safety of nanosized particles in titanium dioxide– and zinc oxide–based sunscreens. Journal of the American Academy of Dermatology 61(4): 685–692.

Patel S, Patel JK (2016) A review on a miracle fruits of *Annona muricata*. Journal of Pharmacognosy and Phytochemistry 5(1): 137–148.

Raj NB, Pavithra Gowda NT, Pooja OS, Purushotham B, Kumar MA, … Boppana SB (2021) Harnessing ZnO nanoparticles for antimicrobial and photocatalytic activities. Journal of Photochemistry and Photobiology 6:100021.

Rajabi S, Ramazani A, Hamidi M, Naji T (2015) *Artemia salina* as a model organism in toxicity assessment of nanoparticles. Daru 23(1): 20.

Rajesh K, Krishnan P, Mani A, Anandan K, Gayathri K, Devendran P (2019) Physical strength and Opto-electrical conductivity of L-Serine Phosphate single crystal for structural and photonics devices fabrica-

tion. Materials Research Innovations.

Ramanarayanan R, Bhabhina NM, Dharsana MV, Nivedita CV, Sindhu S (2018) Green synthesis of zinc oxide nanoparticles using extract of *Averrhoa bilimbi* (L) and their photoelectrode applications. Materials Today: Proceedings 5(8): 16472–16477.

Ramasamy M, Lee J (2016) Recent nanotechnology approaches for prevention and treatment of biofilm-associated infections on medical devices. BioMed Research International 2016: 1851242.

Rasmussen JW, Martinez E, Louka P, Wingett DG (2010) Zinc oxide nanoparticles for selective destruction of tumor cells and potential for drug delivery applications. Expert Opinion on Drug Delivery 7(9): 1063–1077.

Riaz M, Khalid R, Afzal M, Anjum F, Fatima H, … Mtewa AG (2023) Phytobioactive compounds as therapeutic agents for human diseases: a review. Food Science & Nutrition 11(6): 2500–2528.

Rotruck JT, Pope AL, Ganther HE, Swanson AB, Hafeman DG, Hoekstra WG (1973) Selenium: biochemical role as a component of glutathione peroxidase. Science 179(4073): 588–590.

Sabapati M, Palei NN, CK AK, Molakpogu RB (2019) Solid lipid nanoparticles of *Annona muricata* fruit extract: formulation, optimization and in vitro cytotoxicity studies. Drug Development and Industrial Pharmacy 45(4): 577–586.

Silva RM, Silva ID, Estevinho MM, Estevinho LM (2021) Anti-bacterial activity of *Annona muricata* Linnaeus extracts: a systematic review. Food Science and Technology 42.

Somu P, Paul S (2019) A biomolecule-assisted one-pot synthesis of zinc oxide nanoparticles and its bioconjugate with curcumin for potential multifaceted therapeutic applications. New Journal of Chemistry 43(30):11934–11948.

Tamrat E, Asmare Z, Geteneh A, Sisay A, Getachew E, … Reta MA (2025) The global prevalence of biofilm-forming *Enterococcus faecalis* in clinical isolates: a systematic review and meta-analysis. BMC Infectious Diseases 25: 981.

Trestrail C, Nugegoda D, Shimeta J (2020) Invertebrate responses to microplastic ingestion: reviewing the role of the antioxidant system. Science of the Total Environment 734:138559.

Trestrail C, Walpitagama M, Miranda A, Nugegoda D, Shimeta J (2021) Microplastics alter digestive enzyme activities in the marine bivalve, *Mytilus galloprovincialis*. Science of the Total Environment 779:146418.

Veeramani S, Baskaralingam V (2011) Shell-bound iron dependent nitric oxide synthesis in encysted *Artemia parthenogenetica* embryos during hydrogen peroxide exposure. Biometals 24(6):1035–1044.

Vijayakumar S, Vaseeharan B, Malaikozhundan B, Gopi N, Ekambaram P, … Velusamy P (2017) Therapeutic effects of gold nanoparticles synthesized using *Musa paradisiaca* peel extract against multiple antibiotic resistant *Enterococcus faecalis* biofilms and human lung cancer cells (A549). Microbial Pathogenesis 102:173–183.

Vinotha V, Iswarya A, Thaya R, Govindarajan M, Alharbi NS, … Vaseeharan B (2019) Synthesis of ZnO nanoparticles using insulin-rich leaf extract: anti-diabetic, antibiofilm and anti-oxidant properties. Journal of Photochemistry and Photobiology B: Biology 197:111541.

FA Faiz https://orcid.org/0009-0006-0050-8690
R Vijayakumar https://orcid.org/0000-0003-0406-9200